JCI insight

Cardiac fibroblast proliferation rates and collagen expression mature early and are unaltered with advancing age

Rimao Wu, … , Matteo Pellegrini, Arjun Deb

JCI Insight. 2020. https://doi.org/10.1172/jci.insight.140628.

Research In-Press Preview Aging Cardiology

Cardiac fibrosis is a pathophysiologic hallmark of the aging heart. In the uninjured heart, cardiac fibroblasts exist in the quiescent state, but little is known about how proliferation rates and fibroblast transcriptional programs change throughout the lifespan of the organism from the immediate postnatal period to adult life and old age. Using EdU pulse labeling, we demonstrate that more than 50% of cardiac fibroblasts are actively proliferating in the first day of post-natal life. However, within 4 weeks of birth in the juvenile animal, only 10% of cardiac fibroblasts are proliferating. By early adulthood, the fraction of proliferating cardiac fibroblasts further decreases to approximately 2%, where it so remains throughout the rest of the organism's life span. Examination of absolute cardiac fibroblast numbers demonstrated concordance with age related changes in fibroblast proliferation with no significant differences in absolute cardiac fibroblast numbers between animals 14 weeks and 1.5 years of age. We demonstrate that the maximal changes in cardiac fibroblast transcriptional programs and in particular collagen expression occur within the first weeks of life from the immediate postnatal to the juvenile period. We show that even though the aging heart exhibits an increase in the total amount of accumulated collagen, transcription of various collagens and ECM genes both in the heart and cardiac fibroblast is maximal in the newly born and […]

Cardiac fibroblast proliferation rates and collagen expression mature early and are unaltered with advancing age

Rimao Wu[1,2,3,4,5,6], Feiyang Ma[3,4,5], Anela Tosevska[3,5], Colin Farrell[7], Matteo Pellegrini[3,4,5], Arjun Deb*[1,2,3,4,5,6]

[1]Division of Cardiology, Department of Medicine, David Geffen School of Medicine, University of California, Los Angeles, CA 90095.

[2]UCLA Cardiovascular Theme, David Geffen School of Medicine, University of California, Los Angeles, CA 90095

[3]Department of Molecular, Cell and Developmental Biology, College of Life Sciences, University of California, Los Angeles, CA 90095.

[4]Eli & Edythe Broad Center of Regenerative Medicine and Stem Cell Research, University of California, Los Angeles, CA 90095.

[5]Molecular Biology Institute, University of California, Los Angeles, CA 90095.

[6]California NanoSystems Institute, University of California, Los Angeles, CA 90095.

[7]Department of Human Genetics, David Geffen School of Medicine, University of California, Los Angeles, CA 90095

*Correspondence
Arjun Deb, MD
McDonald Research Laboratories 3609A,
675 Charles E Young Drive S,
University of California, Los Angeles, CA 90095
Email: adeb@mednet.ucla.edu
Phone: 310-825-9911

Conflict of interest: The authors have declared that no conflict of interest exists.

Abstract

Cardiac fibrosis is a pathophysiologic hallmark of the aging heart. In the uninjured heart, cardiac fibroblasts exist in the quiescent state, but little is known about how proliferation rates and fibroblast transcriptional programs change throughout the lifespan of the organism from the immediate postnatal period to adult life and old age. Using EdU pulse labeling, we demonstrate that more than 50% of cardiac fibroblasts are actively proliferating in the first day of post-natal life. However, within 4 weeks of birth in the juvenile animal, only 10% of cardiac fibroblasts are proliferating. By early adulthood, the fraction of proliferating cardiac fibroblasts further decreases to approximately 2%, where it so remains throughout the rest of the organism's life span. Examination of absolute cardiac fibroblast numbers demonstrated concordance with age related changes in fibroblast proliferation with no significant differences in absolute cardiac fibroblast numbers between animals 14 weeks and 1.5 years of age. We demonstrate that the maximal changes in cardiac fibroblast transcriptional programs and in particular collagen expression occur within the first weeks of life from the immediate postnatal to the juvenile period. We show that even though the aging heart exhibits an increase in the total amount of accumulated collagen, transcription of various collagens and ECM genes both in the heart and cardiac fibroblast is maximal in the newly born and juvenile animal and decreases with organismal aging. Examination of DNA methylation changes both in the heart and in cardiac fibroblasts did not demonstrate significant changes in differentially methylated regions between young and old mice. Our observations demonstrate that cardiac fibroblasts attain a stable proliferation rate and transcriptional program early in the life span of the organism and suggest a model of cardiac aging where phenotypic changes in the aging heart are not directly attributable to changes in proliferation rate or altered collagen expression in cardiac fibroblasts.

Introduction

The mammalian cardiac muscle cell is highly proliferative within the first few days of birth(1) but subsequently undergoes cell cycle arrest(2) and the myocyte undergoes minimal turnover for the rest for the life of the organism(3). As the organism transitions from the immediate post-natal life to early adulthood and then old age, age related changes occur both in the cellular and extracellular components of the heart. Increased fibrosis or accumulation of extracellular matrix within the heart is a characteristic phenotype of cardiac aging and is associated with age related clinical sequelae such as increasing stiffness of ventricular chambers and abnormalities of myocardial relaxation(4). Cardiac fibroblasts reside in an interstitial position between cardiomyocytes and are the principal cells that secrete extracellular matrix(5). They exist in a quiescent state(6) in the uninjured heart but it is not clear whether fibroblasts exhibit an age dependent increase in proliferation rate, or increase in expression of ECM genes that potentially contributes to age related cardiac fibrosis. In fact, little is known about how cardiac fibroblast proliferation rates and transcriptional programs change from the immediate post-natal period through early adulthood and advanced age.

In this study, we investigate changes in cardiac fibroblast proliferation and transcription throughout the life span of the mouse starting from Day 1 of post-natal life through the early juvenile period (4 weeks), adulthood (14 and 24 weeks) and advanced age (1 and 1.5 years) to determine whether such age dependent dynamic changes in the fibroblast could underlie the phenotype of increased fibrosis in the aging heart. We determined cardiac fibroblast proliferation rates in hearts of mice at different ages by measuring markers of proliferation or by pulse labeling of animals with EdU. Using these corroborative methodologies, we observed that the highest

rates of cardiac fibroblast proliferation were in the immediate post-natal period with subsequent decline in the rates of proliferation across early juvenile and early adulthood periods. By 14 weeks of age, the proliferative rates of cardiac fibroblasts had attained a low steady state of 2-3% and despite advancing organismal aging, no further changes in cardiac fibroblast proliferation were observed. Concordant with age related changes in cardiac fibroblast proliferation rate, we observed that there was no significant difference between the absolute numbers of cardiac fibroblasts between mice 14 weeks and 1.5 years of age. We observed that the composition of the non-myocyte cell population in the neonatal heart differs significantly from that of the juvenile or adult heart. In the neonatal heart, cardiac fibroblasts and not endothelial cells comprised the majority of non-myocyte cells and by early adulthood, with progressive decrease in fibroblast proliferation, endothelial cells formed the majority of the non-myocyte cell fraction and this remained the case with organismal aging. Taken together, these observations demonstrate that cardiac fibroblasts attain a stable proliferation rate early in adulthood and do not exhibit an age dependent increase in proliferation.

Collagens form the major component of the cardiac extracellular matrix and as the aging heart is known to be more fibrotic, we investigated whether changes in fibroblast transcriptional programs and in particular collagen expression increases with age. Cardiac fibroblasts and hearts from which cardiac fibroblasts were isolated were harvested at different ages for gene expression analysis by RNA-seq. Analysis of the expression of all collagens demonstrated that the highest expression of collagen genes occurred in the immediate post-natal period with a progressive decrease in collagen expression in juveniles, adults and mice of advancing age. As epigenetic changes such as DNA methylation have been recently shown to be strong

determinants of biological aging, we examined the degree of DNA methylation in cardiac fibroblasts isolated from early adulthood (14 weeks) and advanced age (1.5 years). We did not observe any significant differences in methylation. Our data suggests that cardiac fibroblasts do not exhibit an age dependent increase in proliferation, collagen expression or DNA methylation. Collectively, these observations demonstrate that age related cardiac phenotypes such as increased fibrosis cannot be directly attributed to altered fibroblast proliferation or increased ECM gene expression.

Results

EdU labeling of fibroblasts in hearts of neonatal, juvenile, adult and old mice

To determine proliferation rates in cardiac fibroblast at various ages in post-natal life, we administered the thymidine analog EdU (5-ethynyl-2'-deoxyuridine) daily for 7 days to pregnant animals (7 days prior to delivery) or animals 4 weeks, 14 weeks, 24 weeks and 1 year old (**Fig 1A**). At the completion of 7 days of daily EdU administration, the animals were euthanized and the hearts harvested and subjected to enzymatic digestion to remove myocytes and isolate the non-myocyte fraction(7). We next subjected the non-myocyte fraction to flow cytometry to determine the fraction of cardiac fibroblasts that retained EdU. As there is no universal marker for cardiac fibroblasts, a panoply of cell surface antigens (Platelet derived growth factor receptor alpha (PDGFRα), MEFSK4, CD90.2 (Thy 1.2)) that are known to be abundantly expressed in cardiac fibroblasts were used for identifying cardiac fibroblasts(8, 9). Flow cytometry demonstrated that on post-natal day 1, 69.70±5.73% of MEFSK4 **(Fig 1B)**, 63.78±4.40% of PDGFRα **(Fig 1C)** and 66.90±2.97% of Thy1.2 **(Fig 1D)** cardiac fibroblasts retained EdU (mean±S.D., n=5 hearts). However by 4 weeks of age, the number of cells that had taken up EdU

during the prior 7 days of administration had dropped to 10.18±3.96% for MEFSK4 cardiac fibroblasts (mean±S.D., n=7 hearts), 7.91±2.80% for PDGFRα (mean±S.D., n=6 hearts) and 7.70±1.54% for Thy1.2 cardiac fibroblasts respectively (mean±S.D., n=11) (**Fig 1B-D**). At 14 weeks [mean±S.D, n=5 (MEFSK4), n=6 (PDGFRα, Thy1.2)] and 24 weeks (mean±S.D., n=5), we observed a further decrease with approximately 2.1 to 5.5% of cardiac fibroblasts being positive for EdU uptake (mean±S.D., n=5). At 1 year of age, the fraction of cardiac fibroblasts that had taken up EdU was 4.30±2.26% for MEFSK4, 1.98±0.57% for PDGFRα and 2.49±0.57% for Thy1.2 (mean±S.D., n=5), and there were no significant differences between the fraction of EdU positive cardiac fibroblasts between 14 weeks, 6 months and 1 year **(Fig 1E-G).** Taken together, these observations suggest that the highest rates of cardiac fibroblast proliferation are observed in the immediate post-natal period and the proliferation rate rapidly declines by the early juvenile period (4 weeks) and significantly declines further to a stable and low level of cardiac fibroblast proliferation by early adulthood (14 weeks) and this remains similar even with advancing organismal age.

Determination of cardiac fibroblast proliferation by assessment of markers of proliferation.

To corroborate our observations with EdU uptake by cardiac fibroblasts, we directly determined expression of markers of proliferation of cardiac fibroblasts. We adopted a similar experimental design and again harvested hearts of animals at post-natal day 1, 4 weeks, 14 weeks, 6 months and 1 year, isolated cardiac fibroblasts and used the same markers to determine the fraction of cardiac fibroblasts expressing Ki67, a marker of proliferation (**Fig 2A**). We observed that the highest rates of proliferation occurred in post-natal Day 1 with 51.93±9% of PDGFRα, 37.53±5.6% of

MEFSK4 and 45.93±7.03% of Thy1.2 cardiac fibroblasts co-expressing Ki67 (mean±S.D., n=6 hearts) (**Fig 2B-D**). These numbers overall agree with the fraction of cardiac fibroblasts that had taken up EdU at post-natal day 1 and suggest that more than half of cardiac fibroblasts are actively proliferating at post-natal Day 1. At 4 weeks of age, 6.55±2.38% of PDGFRα (mean±S.D., n=12 hearts), 13.03±3.11% of MEFSK4 (mean±S.D., n=14 hearts), and 8.13±1.57% of Thy1.2 (mean±SD, n=12 hearts), cardiac fibroblasts co-expressed Ki67 (**Fig 2B-D**)**.** These observations mirror the significant decreases in the fraction of proliferating cardiac fibroblasts from post-natal Day 1 to 4 weeks seen with EdU administration. At 14 weeks of age, the fraction of proliferating cardiac fibroblasts expressing Ki67 had significantly decreased further to between 2.4 and 4.8% [mean±S.D, n=5 (PDGFRα), n=7 (MEFSK4, Thy1.2)] but beyond 14 weeks, the rate of cardiac fibroblast proliferation again remained similar with no significant differences in the fraction of proliferating cardiac fibroblasts between 14 weeks, 6 months and 1 year of age **(Fig 2E-G)**.

Fraction of cardiac fibroblasts comprising the non-myocyte population from post-natal Day 1 to 1 year of age.

We next determined the fraction of cardiac fibroblasts comprising the cardiac non-myocyte cell population. Emerging evidence suggests that cardiac fibroblasts in the adult animal comprise approximately 20% of the non-myocyte fraction with endothelial cells comprising the vast majority of non-myocytes in the adult heart(9). We performed flow cytometry for endothelial marker (CD31) and observed that CD31 expressing cells comprised only 30.87±2.15% of non-myocyte cells at post-natal day 1 (mean±S.D., n=10 hearts) but the fraction of endothelial cells by 4 weeks had increased to approximately 69.83±9.24% of the non-myocyte population (mean±SD, n=10 hearts) and remained approximately close to 65% at 14 weeks, 24 weeks and

1 year (**Fig 3A,E**). Our data is consistent with recent reports that endothelial cells represent the predominant non-myocyte population in the adult heart(9). By contrast, the population of PDGFRα expressing fibroblasts as a fraction of the non-myocyte population was approximately 45.60±12.27% at post-natal Day 1 (mean±SD, n=10 hearts) but had decreased to 29.78±9.82% at 4 weeks (mean±SD, n=23 hearts) and remained between 25 and 30% of the non-myocyte population in adults and mice of advancing age (**Fig 3B,F**). The fraction of Thy1.2 and MEFSK4 cells comprising the non-myocyte fraction did not change significantly from neonatal to adult life and beyond suggesting that cardiac fibroblasts identified by PDGFRα expression undergo the most dynamic changes in numbers from neonatal life to adulthood (**Fig 3C,D,G,H**). Our observations demonstrate that the composition of the non-myocyte cell population of the neonatal heart is significantly different from that observed in the adult heart, but by 4 weeks of age, the cellular composition of cardiac non-myocytes is very similar to that in the adult heart and the fraction of cardiac fibroblasts constituting the non-myocyte fraction does not significantly change with advancing age (**Fig 3E-H**) (mean±S.D., n=10 hearts).

Next, we examined the absolute numbers of cardiac fibroblasts in hearts of mice from the neonatal period to old age to determine whether the changes in the absolute numbers of cardiac fibroblasts were concordant with age dependent changes in cardiac fibroblast proliferation rates. To determine the absolute numbers of cardiac fibroblasts, we harvested whole heart tissue from animals aged post-natal day 1 to 1.5 years of age, isolated the cardiac fibroblasts by expression of MEFSK4, Thy1.2 and PDGFRα and normalized the number of cardiac fibroblasts to the total number of cells in unit weight of heart tissue as described(10). We observed that the number of MEFSK4, Thy1.2 and PDGFRα cardiac fibroblasts at 4 (mean±SD, n=20

hearts) and 14 weeks (mean±SD, n=21 hearts) of age was significantly greater than those in the hearts of post-natal day 1(mean±SD, MEFSKF n=21; Thy1.2 n=26; PDGRFα N=20 hearts) animals and 4 week old animals respectively (**Fig 4A-C**). However, there was no significant difference in absolute cardiac fibroblast numbers between animals 1.5 years (mean±SD, n=14 hearts) of age and 14 weeks of age with the absolute numbers of PDGFRα cardiac fibroblasts demonstrating a slight but significant decrease at 1.5 years compared to 14 weeks. **(Fig4A-C)**. These data are thus concordant with the age dependent changes in cardiac fibroblast numbers we have observed. Cardiac fibroblasts are highly proliferative in the immediate post-natal period and remain proliferative at 4 weeks of age, albeit at a lower proliferative rate and thus the absolute numbers of cardiac fibroblasts are higher at 4 weeks compared to post-natal day 1 and at 14 weeks compared to that at 4 weeks. However the proliferation rate declines thereafter and remains stable for the rest of the life of the organism and hence absolute cardiac fibroblast numbers do not change significantly thereafter with age.

We also investigated whether there were gender specific differences in absolute cardiac fibroblast proliferation rates. Examination of the absolute numbers of MEFSK4 expressing cardiac fibroblasts did not show any differences between male and female mice at post-natal day 1, 4 week, 14 week or 1.5 years (**Supplementary Figure 1A**). Similarly there were no differences in the proliferation rates of Thy1.2 expressing cardiac fibroblasts (as measured by Edu uptake) between male and female animals at different ages (**Supplementary Figure 1B**).

Gene expression changes in cardiac fibroblasts and the heart from postnatal to advanced age.

As the heart ages, there is accumulation of extracellular matrix or fibrosis that is

considered to be characteristic phenotype of cardiac aging. As cardiac fibroblasts do not exhibit an age dependent increase in proliferation, we next investigated how the transcriptional program of cardiac fibroblasts changes from immediate post-natal life to advanced age. For this purpose, we harvested hearts from post-natal day 1 old animals as well as from 4 week, 14 week, 1 year and 1.5 years old animals. Cardiac fibroblasts were isolated by expression of PDGFRα expression and both cardiac fibroblasts and the hearts from which they were so isolated were subjected to gene expression analysis by RNA-seq. First, we analyzed differentially expressed genes (DEGs) among PDGFRα expressing cardiac fibroblasts from across all ages (i.e. from post-natal day 1 to 1.5 years) and performed weighted gene correlation network analysis (WGCNA) to find modules of genes highly correlated with advancing age. (**Fig 5A**). Out of the modules described, we observed that the genes in module 3 (M3) and module 17 (M17) exhibited the strongest correlation with advancing age (**Fig 5B**). M3 represented a cluster of genes that was progressively down-regulated with advancing age and gene ontology analysis demonstrated genes associated with cell cycle and DNA replication to be predominantly down-regulated consistent with our observations of decreased cell proliferation of cardiac fibroblasts with age (**Fig 5C, Table 1**). A smaller cluster of genes (M17) demonstrated age dependent increase in expression in cardiac fibroblasts and represented genes regulating metabolic pathways, MAPK and inflammation (**Fig 5D, Table 2**). A similar analysis of genes that correlate with advancing age in the whole heart demonstrated a module of genes (M1) to be progressively downregulated with age (**Fig 6A,B**) and this contained a diverse set of genes regulating cellular and organelle organization, protein modification and associated metabolic processes (**Fig 6C, Table 3**). Clusters of genes that show progressive upregulation with advancing age (Module 17) in the

whole heart included genes that regulated mitochondrial function including electron transport chain, ATP synthesis and mitochondrial organization (**Figure 6D, Table 4**).

As the aging heart is known to be more fibrotic, we determined expression of collagens in the heart as well in PDGFRα fibroblasts isolated from animals aged post-natal day 1 to 1.5 years. We observed that the expression of most collagen genes including the genes for the principal collagens Col I (Col1a1, Col1a2, Col1a3) and Col III (Col3a1) significantly decreased from the neonatal period to 4 weeks and beyond (**Fig 5E**). Only genes encoding for Col IV, a collagen present in the basement membrane of blood vessels showed increased expression from post-natal day 1 to 4 weeks of age, consistent with our observations of more endothelial cells at 4 weeks of age (**Fig 5E**). Analysis of collagen expression in the whole heart mirrored that of in cardiac fibroblasts with the principal collagen encoding genes for Col1 and Col III exhibiting the highest expression in post-natal day 1 and undergoing downregulation of expression with age (**Fig 5F**). We examined the total collagen content of hearts and consistent with previously made observations of increased collagen content in the aging heart(11), we observed that the 1.5 year old heart had 51% more collagen than the 1 day old heart (69.3±9.01μg/mg in 1.5 year old hearts (n=11) vs 45.7±8.3 μg/mg in post-natal day 1 hearts (n=9), mean±S.D) (**Figure 6E**). These data thus suggest that even though collagen expression in the heart and the cardiac fibroblasts significantly decreases with age, the heart accumulates collagen protein with age. Nascent collagen undergoes cross linking with age and cross linked collagen is resistant to breakdown by collagenases or other matrix metalloproteinases(12). We examined age related changes in gene expression in both cardiac fibroblasts and the heart to determine if there were any patterns in expression of metalloproteinases (MMPs), tissue inhibitors of metalloproteinases

(TIMPs) or gene regulating cross linking (Lysyl oxidase). We observed that several MMPs such as MMP3 and MMP 19 as well as TIMP 1 and 2 demonstrated significant increased expression in older mice compared to younger animals (**Supplementary Figure 2A,B**). However no significant pattern was obvious with downregulation of both members of the MMP and TIMP family in both cardiac fibroblasts and hearts of older mice compared to younger animals (**Supplementary Figure 2A,B**). As the TGF-β pathway is known to be a critical regulator of fibrosis, we examined expression of genes in the TGF-β pathway and observed decreased age dependent decrease in Smad1 and TGFBR 1expression in both the heart and cardiac fibroblasts but no obvious pattern was again evident with increased expression of other members of the TGF, SMAD and BMP family (**Supplementary Figure 2C,D**). We also looked at expression of lysyl oxidase (LOX), which regulated cross linking of extracellular matrix and observed significant downregulation of gene expression with age both in the heart and in cardiac fibroblasts with age (**Supplementary Figure 2E,F**). These data likely suggest that as cross linking occurs with age, LOX expression is downregulated. Taken together these data suggest that the accumulation of collagen in the aging heart is thus not directly linked to increased collagen expression or increased numbers of cardiac fibroblasts but likely represent mechanisms of decreased turnover owing to cross linking or decreased proteolysis.

Epigenetic changes such as changes in DNA methylation have been recently considered strong indicators of aging in a variety of tissues(13). Our data demonstrates that cardiac fibroblast proliferation rates as well as transcription programs become stable by 14 weeks and do not undergo any further changes. We next determined the DNA methylation status of PDGFRα expressing cardiac

fibroblasts and whole hearts harvested from animals 14 weeks and 1.5 years old respectively. We examined the differentially methylated regions (DMRs) with respect to hypo/hypermethylation and binned them according to distance from transcription start sites (TSS). More than 2500 regions in the genome of cardiac fibroblasts harvested at these two ages exhibited at least 10% difference in methylation. However, the number of regions that exhibited at least 20% differences in the degree of methylation dropped to less than 100 and applying a stringent criterion of FDR<0.1, we observed very few regions exhibiting any differences (**Fig 5G**). Examination of DMR in the whole heart tissue of 14 week and 1.5 year old animals also mirrored observations seen in cardiac fibroblasts and there were minimal differences in the DMRs when stringent statistical criteria were employed (**Fig 5H**). These observations demonstrate that even with advancing age, the methylation status of the genome of both cardiac fibroblasts and the heart does not appreciably change beyond 14 weeks of age.

Discussion

Our data illustrates the dynamics of fibroblast proliferation and transcriptional programs from early post-natal life to advanced age. The aging heart is known to have a greater amount of fibrotic tissue, but fibroblast proliferation rates are the greatest in the neonatal period and rapidly decline thereafter. These observations are consistent with prior observations demonstrating that fibroblast proliferation rates rapidly decline within the first few weeks of post-natal life(14). Fibroblast numbers calculated as the fraction of non-myocyte cells or even absolute cardiac fibroblast numbers did not significantly differ in young and old hearts and thus changes in fibroblast proliferation likely do not directly underlie increased fibrosis seen with aging. We used antigens abundantly expressed in cardiac fibroblasts to identify

broad populations of cardiac fibroblasts in the heart, and although age dependent proliferation rates were similar in the fibroblast populations examined, it is possible that subsets of cardiac fibroblasts within these populations or others not examined by us could differ in age dependent biological properties. Consistent with age dependent decline or stabilization of low proliferation rates, expression of key collagen genes is the highest in the neonatal period and stabilizes to a low rate by early adulthood suggesting that fibroblasts maintain a quiescent fibrotic program throughout life that is stable from early adulthood. Mechanisms of age dependent fibrosis are poorly understood(15) but the increased amount of extracellular matrix in the aging heart cannot be directly attributed to increased fibroblast proliferation rates or increased expression of collagens and likely results from the decreased breakdown of collagen as collagen gets more cross linked and more resistant to proteolysis. In this regard, we observed that Lox expression decreased from the neonatal to the adult mouse and could reflect decreased expression of the gene as the matrix gets more cross linked. Whether the increased accumulation of collagen in the aging heart exerts a negative feedback effect on cardiac fibroblasts to decrease collagen expression is not clear from our study. Rather than being a cell that contributes to increased collagen deposition with age, our data suggests that the cardiac fibroblast by decreasing collagen expression and lowering proliferation rates from early adulthood to advanced age potentially plays a protective role in preventing excessive fibrosis of the heart with organismal aging.

Methods

All experiments were approved by the Animal Research Committee at the University of California, Los Angeles. A full description of methods is provided in the accompanying supplementary file.

Isolation of non-myocyte population from the heart

C57Bl/6 mice of different ages from post-natal day 1 to 1.5 year and hearts harvested at specific ages as outlined in the manuscript. The ventricles were used for isolation of non-myocyte cells following removal of the atria and the heart valves. The hearts were rinsed in ice cold HBSS chopped into 1mm square pieces, suspended in 0.1µg/ml liberase TH (Roche, 5401151001) in Tyrodes buffer (136mM NaCl, 5.4mM KCl, 0.33mM NaH2PO4, 1mM MgCl2, 10mM HEPES, 0.18% Glucose), and subsequently placed in a shaking incubator at 37˚C for 30 min at 80 rpm. Digested hearts were filtered with a 40µm cell strainer (Fisher, 22363547), centrifuged at 200g for 5 min, and non-myocyte cell resuspended with 10ml of 1% BSA.

Flow cytometry for fibroblast and endothelial antigens, EdU uptake and Ki67 expression

C57Bl/6 animals were used for all experiments. For determination of EdU incorporation, either pregnant animals (7 days prior to birth of pups) or animals at 4 weeks, 14 weeks, 24 weeks and 1 year age were administered EdU daily (Carbosynth, NE0870) at 50 mg/kg for seven consecutive days. Following completion of EdU administration, animals were euthanized and hearts harvested for isolation of non-myocyte cells. For identification of cardiac fibroblasts, $2X10^6$ non-myocytes suspended in 100 ul 1% BSA in PBS were incubated for 30 minutes with

fluorophore conjugated antibodies targeting antigens abundantly present in cardiac fibroblasts MEFSK4-APC (1:20, Miltenyi Biotec 130-102-302), PDGFRα-APC (1:20, eBioscience 17-1401-81) and Thy1.2-APC (1:200 eBioscience 17-0902-82). For identification of endothelial cells, non-myocyte cells were incubated with CD31-APC (1:50, eBioscience 17-0311-82). For identification of EdU uptake, the Click-iT™ Edu Alexa Fluor 488 flow cytometry assay kit (Invitrogen, C10425) was used according to the manufacturer's instructions and flow cytometry performed to identify MEFSK4, PDGFRα and Thy1.2 non-myocyte cell fractions that also were positive for EdU uptake. For identification of cardiac fibroblasts that also co-expressed Ki67 (1:200, eBioscience 11-5698-82), the non-myocyte fraction was first stained with MEFSK4 and then followed by fixation with 4% PFA, permeabilization (eBioscience, 00-8333-56) and staining for Ki67. For PDGFRα and Thy1.2, the cells were fixed and permeabilized first, stained with Ki67 and then followed by staining for surface markers. BD LSRII flow cytometer was used for all flow cytometry experiments. Data was analyzed using Flowjo software. A summary of reagents has been presented in **Supplementary Table 1**.

Quantitation of absolute numbers of cardiac fibroblasts

Absolute numbers of cardiac fibroblasts were determined using a bead based quantification assay as described. The non-myocyte cell population was isolated as described above. All cells were then resuspended in 1% BSA in PBS and then the cellular suspension was spiked with Calibration Particles (Sphero 556298) at a concentration of 1000 beads/mg of absolute tissue weight (measured before processing). Cardiac fibroblasts were identified by staining with fluorescence-conjugated cardiac fibroblast antibodies against specific cell specific antigen markers. Invitrogen Attune NxT Flow Cytometer was used to count the cell number Data

analysis by FlowJo. Calculation of absolute cell numbers was done as follows using equations 1 and 2 below using the beads/volume of tissue for normalization as described(10).

$$\frac{\#\text{ of gate cells}}{\#\text{ of gated beads}} \times \frac{\text{Total beads added to sample}}{\text{Mass of sample (mg)}} = \text{cells/mg.tissue} \quad (1)$$

$$\text{Absolute cell number} = \text{Cells/mg.tissue} \times \text{Tissue weight} \quad (2)$$

Total collagen assay

Assessment of collagen content in post-natal day 1 and 1.5 year old hearts was performed by using Sircol Soluble Collagen Assay Kit (Biocolor, S1000) and Sircol Insoluble Collagen Assay Kit (Biocolor, S2000) to determine total collagen content. Tissues were weighed and homogenized in 0.1mg/ml pepsin/0.5M acetic acid and subsequently incubated overnight at 4˚C in the same buffer. Lysates were centrifuged at 12000 g for 10min. Supernatants were used to measure soluble collagen, and precipitates were used to detect insoluble collagen. For soluble collagen, the supernatants were transfer to new tubes, mixed with 1ml of Sircol Dye Reagent and incubated for 30 min with gentle shaking. Precipitates were washed with 750µl of ice-cold Acid-Salt Wash Reagent. Washed precipitates were dissolved in 500µl of Alkali Reagent, and 200ul of each sample was add to a 96 well plate, and absorbance measured at 550nm using Synergy H1 microplate reader (BioTeK). Soluble collagen standards were added to create a standard curve for quantitative readouts. For determination of insoluble collagen, tissue precipitates were incubated with Fragmentation Reagent at 65˚C for 2 h with vigorous mixing by vortexing every 30 mins to convert insoluble collagen to soluble collagen. Samples so treated were centrifuged at 12000 g for 10 min, and supernatants were transferred into new tubes.

and collagen content estimated as for soluble collagen.

Determination of gene expression changes in cardiac fibroblasts and hearts isolated from animals from post-natal day 1 to 1.5 years

Animals post-natal day 1, 4 weeks, 14 weeks, 1 year and 1.5 years old were used for determination of gene expression analysis. PDGFRα cardiac fibroblasts were isolated by flow cytometry from hearts of animals at the above respective ages to determine changes in gene expression in cardiac fibroblasts. RNA was isolated from the heart tissue or cardiac fibroblasts using RNeasy Mini kit (Qiagen) and used to generate RNA-Seq libraries followed by sequencing using Illumina 4000 platform (single-end, 65bp). The reads were mapped with STAR 2.5.3a (16) to the mouse genome (mm10). The counts for each gene were obtained by using –quantMode GeneCounts commands in STAR, and the other parameters during alignment were set to default. Differential expression analyses were carried out using DESeq2 (17). Normalized counts were obtained using the DESeq2 rlog function with default parameters. Three animals/timepoint and three different sets of PDGFRα fibroblasts isolated from different hearts at each time point were used for differential expression analysis.

Module analysis of correlation networks was performed using Weighted Gene Correlation Analysis (WGCNA)(18). The rlog transformed counts from DESeq2 were used in the WGCNA analysis. A signed gene correlation network was constructed using the with a soft thresholding power of 10. The module eigengene, which represents a linear combination of genes that capture a large fraction of variance in each module, was used to calculated correlation with each time. The modules with the most positive and negative correlation were retained, and genes in these modules were used for enrichment analysis by g:Profiler(19). The accession number

for the RNA sequencing data described in this study is GEO: GSE160074

DNA methylation analysis

Hearts of 14-week-old and 1.5 year old animals were used for determination of differences in DNA methylation of either PDGFRα cardiac fibroblasts isolated from those hearts or whole heart tissue. DNA was first extracted from whole hearts or cardiac fibroblasts (Qiagen All prep DNA/RNA mini kit, Catalog 80204) and then subjected to reduced representation bisulfite sequencing (RRBS) using Illumina NovaSeq SP platform (pair-end, 150bp). Reads were aligned against the mouse genome mm10 using BiSulfite Bolt (BSBolt) [https://bsbolt.readthedocs.io/en/latest/], followed by methylation calling. Methylation matrix was constructed using only CpG sites with at least 10x coverage across at least 80% of the samples. Differentially methylated regions were defined using metilene v02-8(20), Differentially methylated regions were defined as regions with at least 3 CpG sites and at least 10% of methylation difference between comparisons at p-value < 0.05 in the Mann Whitney U test. The Benjamini-Hochberg procedure was used to adjust the false discovery rate. HOMER v4.11(21) was used for DMR annotation to the human genome (hg38). The accession number for the DNA methylation sequencing data described in this study is GEO: GSE160074

Statistics

All statistical analyses and graphical analyses were performed using GraphPad Prism 8. Data are presented as mean ± SD, significant differences between groups were calculated using 2-tailed Student’s t test. Analysis of differences between more than 2 groups was performed using a 1-way ANOVA with multiple-comparisons correction in GraphPad. A p value less than 0.05 was considered significant.

Study approval

All experiments were approved by the Animal Research Committee at the University of California, Los Angeles. A full description of methods is provided in the accompanying supplementary file.

Author contributions

RW performed all experiments, FM analyzed RNA-seq data, AT and CF analyzed DNA methylation data, MP oversaw RNA-seq and methylation data analysis, AD conceptualized the project, supervised data collection and analysis and wrote the manuscript.

Acknowledgements

We thank the UCLA flow cytometry core and the UCLA Technology Center for Genomics and Bioinformatics for assistance with experiments. We thank Dr. Kenneth Dorshkind, UCLA for providing key reagents. This work was funded by grants (HL149687, HL149658, HL137241, AR075867) from the National Institutes of Health and grants (W81XWH-17-1-0464, W81XWH-20-1-0238) from the Department of Defense.

References

1. Porrello ER, et al. Transient regenerative potential of the neonatal mouse heart. *Science.* 2011;331(6020):1078-80.
2. Puente BN, et al. The oxygen-rich postnatal environment induces cardiomyocyte cell-cycle arrest through DNA damage response. *Cell.* 2014;157(3):565-79.
3. Bergmann O, et al. Evidence for Cardiomyocyte Renewal in Humans. *Science.* 2009;324(5923):98-102.
4. Biernacka A, and Frangogiannis NG. Aging and Cardiac Fibrosis. *Aging Dis.* 2011;2(2):158-73.
5. Frangogiannis NG. The extracellular matrix in myocardial injury, repair, and remodeling. *J Clin Invest.* 2017;127(5):1600-12.
6. Tallquist MD. Cardiac Fibroblast Diversity. *Annu Rev Physiol.* 2020;82:63-78.
7. Ubil E, et al. Mesenchymal-endothelial transition contributes to cardiac neovascularization. *Nature.* 2014;514(7524):585-90.
8. Ivey MJ, and Tallquist MD. Defining the Cardiac Fibroblast. *Circ J.* 2016;80(11):2269-76.
9. Pinto AR, et al. Revisiting Cardiac Cellular Composition. *Circ Res.* 2016;118(3):400-9.
10. Reeves RK, et al. Quantification of mucosal mononuclear cells in tissues with a fluorescent bead-based polychromatic flow cytometry assay. *J Immunol Methods.* 2011;367(1-2):95-8.
11. Meschiari CA, Ero OK, Pan H, Finkel T, and Lindsey ML. The impact of aging on cardiac extracellular matrix. *Geroscience.* 2017;39(1):7-18.
12. Lopez B, et al. Myocardial Collagen Cross-Linking Is Associated With Heart Failure Hospitalization in Patients With Hypertensive Heart Failure. *J Am Coll Cardiol.* 2016;67(3):251-60.
13. Horvath S, and Raj K. DNA methylation-based biomarkers and the epigenetic clock theory of ageing. *Nat Rev Genet.* 2018;19(6):371-84.
14. Ivey MJ, Kuwabara JT, Pai JT, Moore RE, Sun Z, and Tallquist MD. Resident fibroblast expansion during cardiac growth and remodeling. *J Mol Cell Cardiol.* 2018;114:161-74.
15. Horn MA, and Trafford AW. Aging and the cardiac collagen matrix: Novel mediators of fibrotic remodelling. *J Mol Cell Cardiol.* 2016;93:175-85.
16. Dobin A, et al. STAR: ultrafast universal RNA-seq aligner. *Bioinformatics.* 2013;29(1):15-21.
17. Love MI, Huber W, and Anders S. Moderated estimation of fold change and dispersion for RNA-seq data with DESeq2. *Genome Biol.* 2014;15(12):550.
18. Langfelder P, and Horvath S. WGCNA: an R package for weighted correlation network analysis. *BMC Bioinformatics.* 2008;9:559.
19. Reimand J, Kull M, Peterson H, Hansen J, and Vilo J. g:Profiler--a web-based toolset for functional profiling of gene lists from large-scale experiments. *Nucleic Acids Res.* 2007;35(Web Server issue):W193-200.
20. Juhling F, Kretzmer H, Bernhart SH, Otto C, Stadler PF, and Hoffmann S. metilene: fast and sensitive calling of differentially methylated regions from bisulfite sequencing data. *Genome Res.* 2016;26(2):256-62.
21. Heinz S, et al. Simple combinations of lineage-determining transcription factors prime cis-regulatory elements required for macrophage and B cell identities. *Mol Cell.* 2010;38(4):576-89.

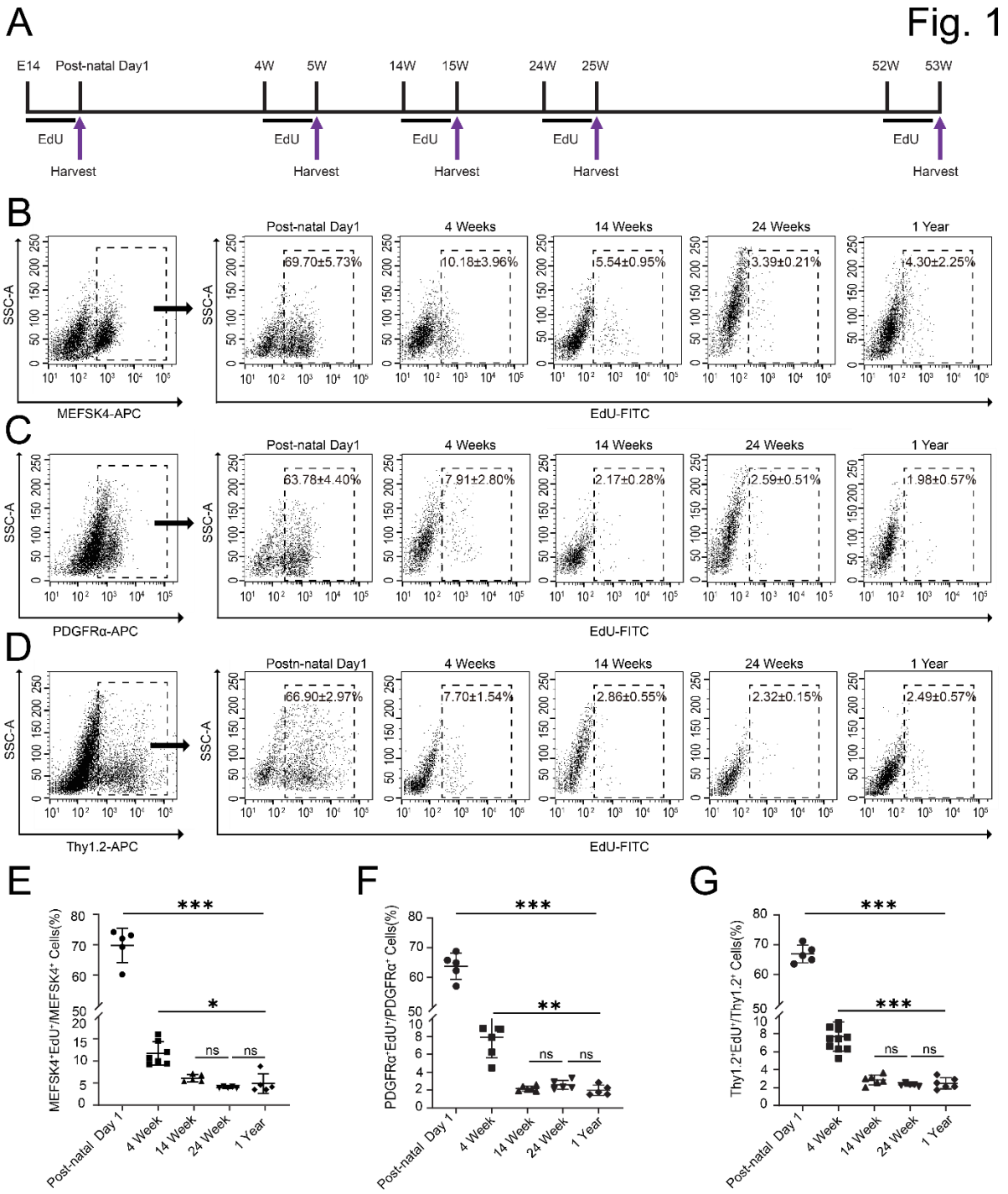

Figure 1. Cardiac fibroblast proliferation with advancing age assessed by EdU incorporation. (A) Experimental outline denoting timing of EdU administration and subsequent harvest 7 days later. **(B-D)**. Non-myocyte cell fraction was first flow-sorted according to expression of **(B)** MEFSK4, **(C)** PDGFRα **(D)** Thy 1.2 and EdU uptake determined in each isolated fraction at each time point (post-natal Day 1, 4 weeks, 14 weeks, 24 weeks and 1 year). Quantitation of **(E)** MEFSK4, **(F)** PDGFRα **(G)** Thy1.2 cardiac fibroblasts that take up EdU at different ages. Post-natal day 1 value is compared to each value at 4,14,24 weeks and 1 year respectively. 4 week value is similarly compared to each value at 14, 24 weeks and 1 year. (mean ± S.D.; *** $p<0.0001$, ** $p<0.01$, * $p<0.05$, ns= $p>0.05$). Data analysis were performed by 1-way ANOVA with multiple-comparisons correction.

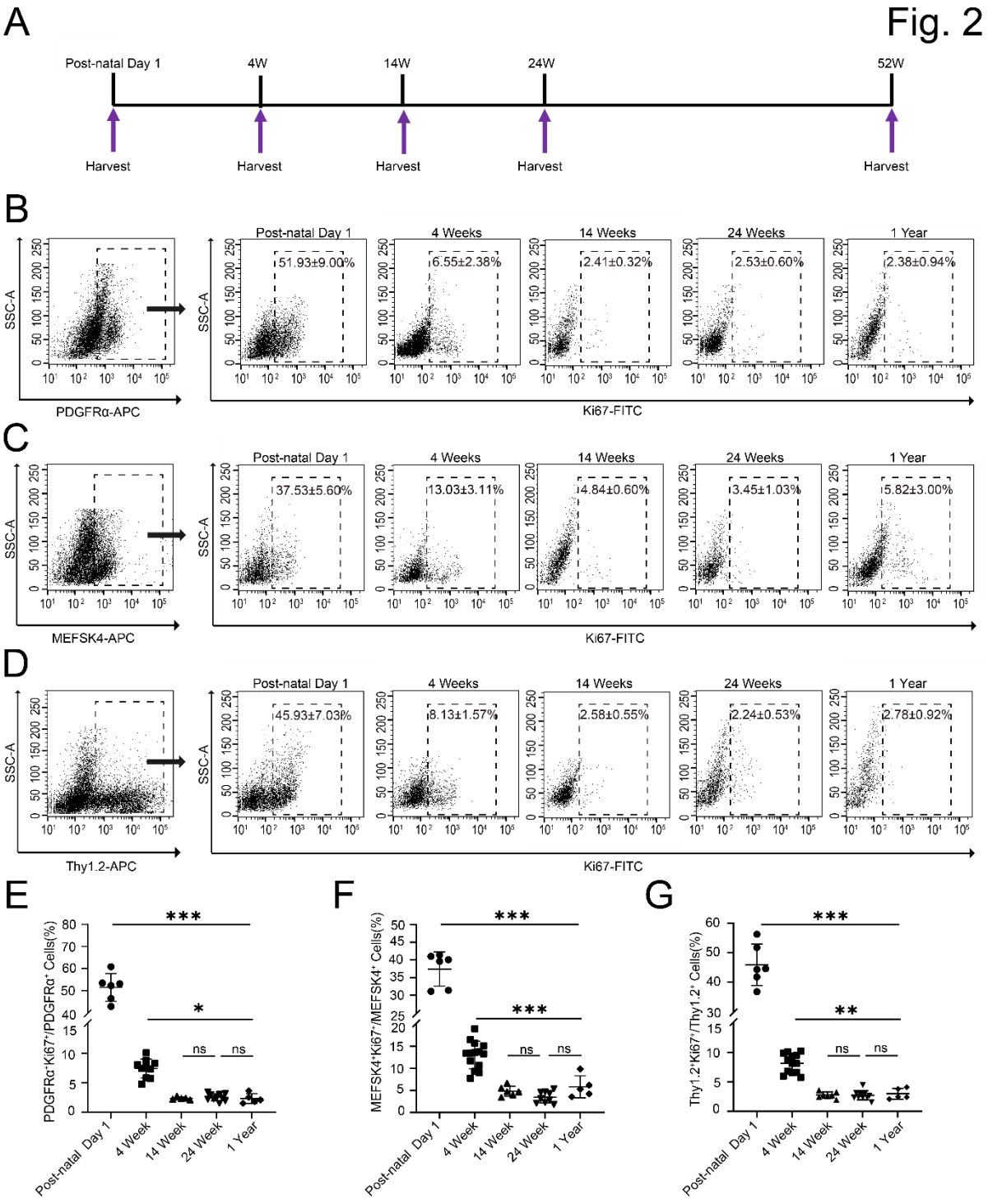

Figure 2. Cardiac fibroblast proliferation with advancing age assessed by Ki67 co-expression. (A) Schematic depicting timing of harvest of heart for cardiac fibroblast isolation **(B-D)** Cardiac fibroblasts were sorted from the non-myocyte cell population by flow sorting for **(B)** PDGFRα **(C)** MEFSK4 and **(D)** Thy 1.2 and Ki67 expression in each of those fractions determined by flow cytometry at post-natal Day 1, 4 weeks, 14 weeks, 24 weeks and 1 year). Quantitation of **(E)** PDGFRα **(F)** MEFSK4 and **(G)**Thy 1.2 cardiac fibroblasts that co-expressed Ki67 at different ages. Post-natal day 1 value is compared to each value at 4,14,24 weeks and 1 year respectively. 4 week value is similarly compared to each value at 14, 24 weeks and 1 year. (mean ± S.D.; *** P<0.0001, **p<0.01, *p<0.05, ns= p>0.05). Data analysis was performed by 1-way ANOVA with multiple-comparisons correction.

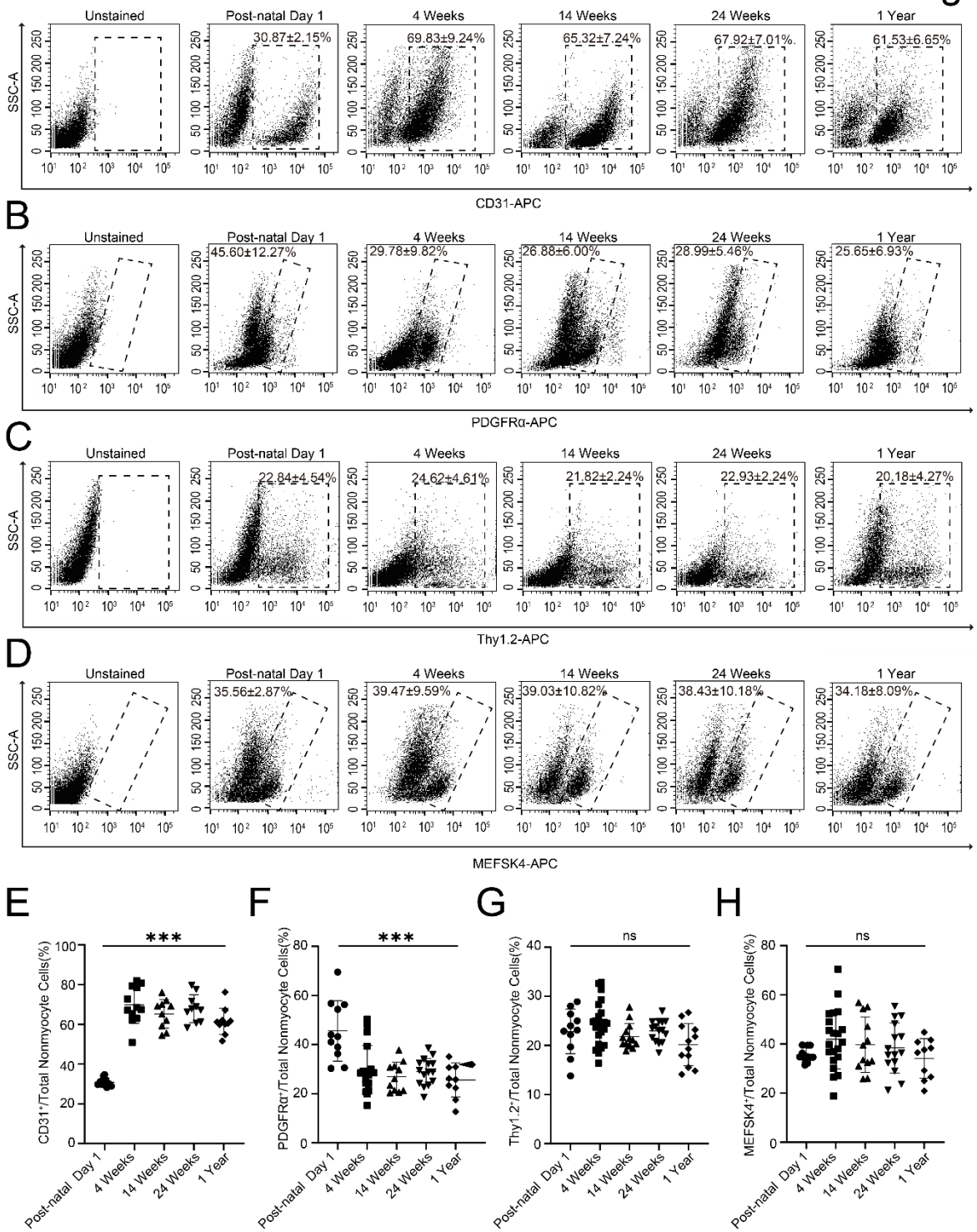

Figure 3. Changing composition of the non-myocyte fraction with advancing age. Non-myocyte cells were isolated from hearts of animals post-natal day 1, 4 weeks, 14 weeks, 24 weeks and 1 year old and subjected to flow cytometry to determine the endothelial and cardiac fibroblast population at these time points. **(A-D)** Flow cytometry demonstrating fraction of non-myocytes staining for **(A)** CD31 (endothelial) **(B)** PDGFRα **(C)** Thy1.2 and **(D)** MEFSK4 and **(E-H)** Quantitation of **(E)** CD31 **(F)** PDGFRα **(G)**Thy1.2 and **(H)** MEFSK4 expressing cells as a fraction of the entire non-myocyte population isolated from the hearts at those time points. Post-natal day 1 value is compared to each value at 4,14,24 weeks and 1 year respectively. (mean ± S.D.; ***p<0.0001, ns= p>0.05). Data analysis was performed by 1-way ANOVA with multiple-comparisons correction.

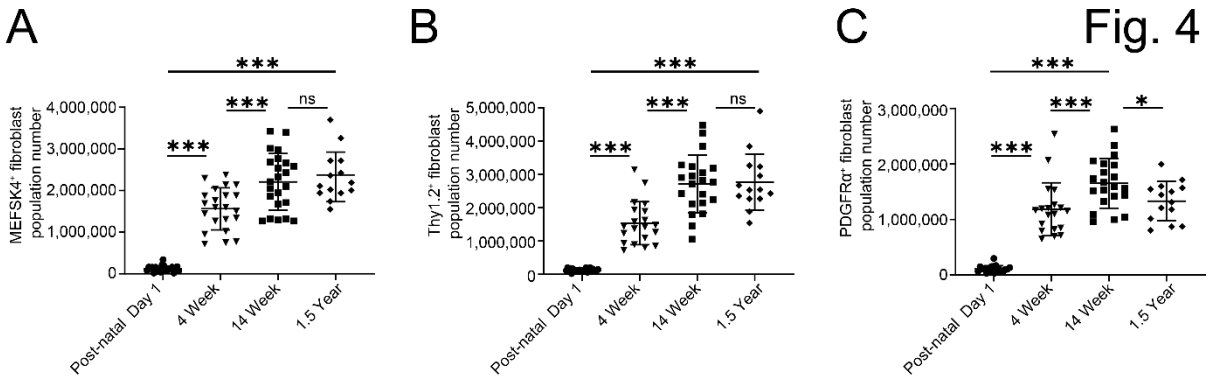

Figure 4. Absolute cardiac fibroblast numbers in hearts of mice determined by beads based flow cytometry. Quantitation of absolute numbers of **(A)** MEFSK4, **(B)** Thy1.2 and **(C)** PDGFRα cardiac fibroblasts in hearts of post-natal day 1, 4 weeks, 14 weeks and 1.5 years of age. (mean ± S.D.; *** $p<0.0001$, *$p<0.05$, ns= $p>0.05$). Data analysis was performed by 1-way ANOVA with multiple-comparisons correction.

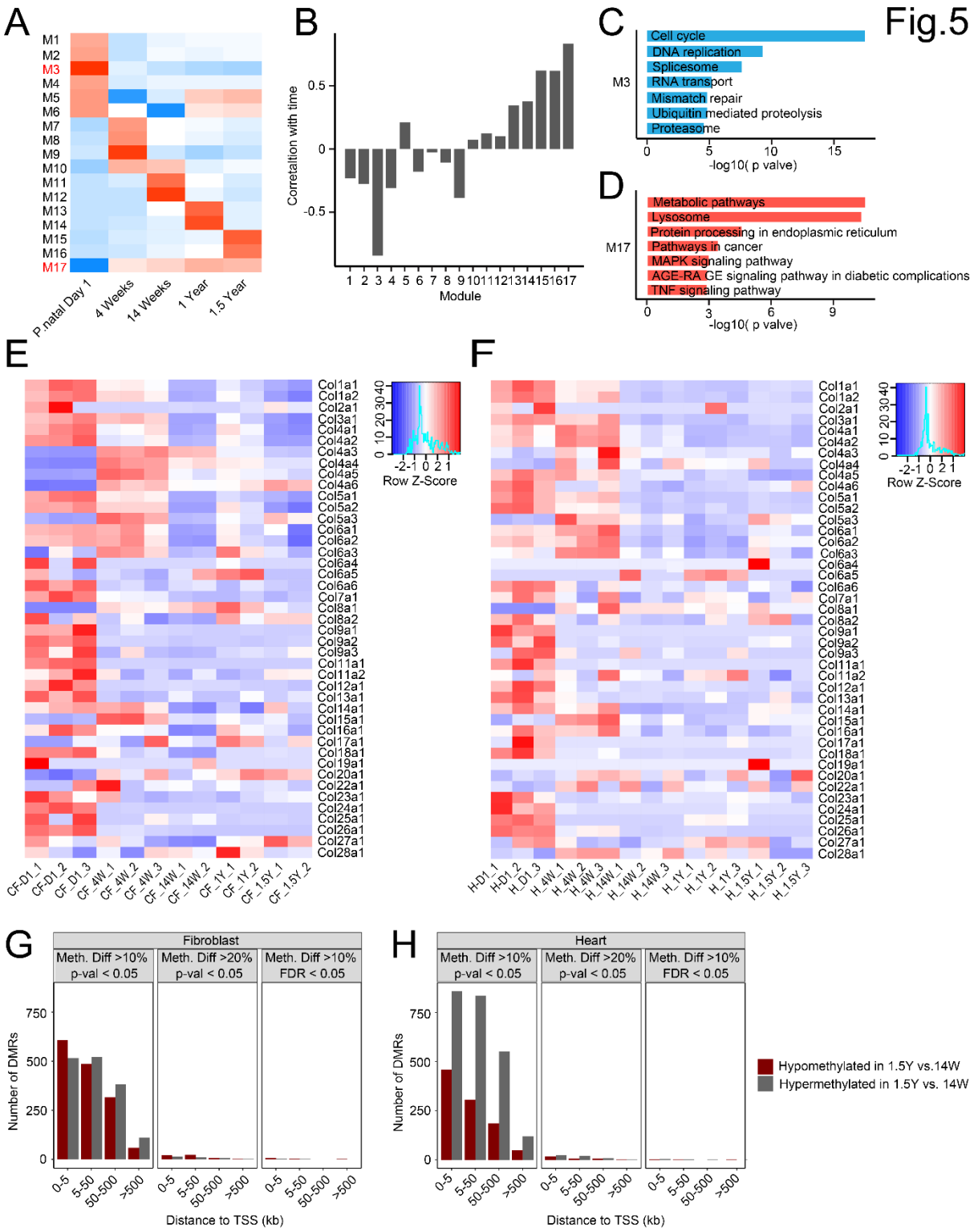

Figure 5. Transcriptional programs and DNA methylation of cardiac fibroblasts and heart with advancing age. Hearts were harvested from post-natal day 1, 4 weeks, 14 weeks, 1 year and 1.5 year old animals and the heart tissue as well as PDGFRα fibroblasts isolated from those hearts were subjected to gene expression analysis by RNA seq. **(A)** Weighted Gene Co-expression Network Analysis of Genes (WGCNA) was performed to identify modules of genes that correlated with time and a heat map demonstrates mean expression of these modules of genes with age **(B)** Graphical representation demonstrating correlation of each module with time **(C,D)** Gene ontology analysis demonstrating principal pathways/biological

processes that are **(C)** downregulated or **(D)** upregulated with age **(E,F)** Heat map demonstrating changes in expression of all collagen encoding genes with age in **(E)** cardiac fibroblasts (PDGFRα+) and **(F)** whole heart tissue **(G,H)** Barplot showing the number of differentially methylated regions (DMRs) between **(G)** cardiac fibroblasts (PDGFRα+) and **(H)** hearts of 1.5 years and 14week old animals, binned by the absolute distance to the nearest transcription start site (TSS); DMRs (hyper and hypomethylated) are shown both in fibroblasts and whole heart tissue. Left panel shows regions with at least 10% difference in methylation between 1.5year and 14week samples and a p-value < 0.05 (Mann Whitney U-test); middle panel shows regions with at least 20% difference in methylation between 1.5year and 14 week samples and a p-value < 0.05 (Mann Whitney U-test); right panel shows number of sites that are retained after adjusting for false discovery rate (FDR < 0.1) with a minimum of 10% difference in methylation between 1.5year and 14 week samples (n=3 hearts or 3 sets of cardiac fibroblasts for each time point).

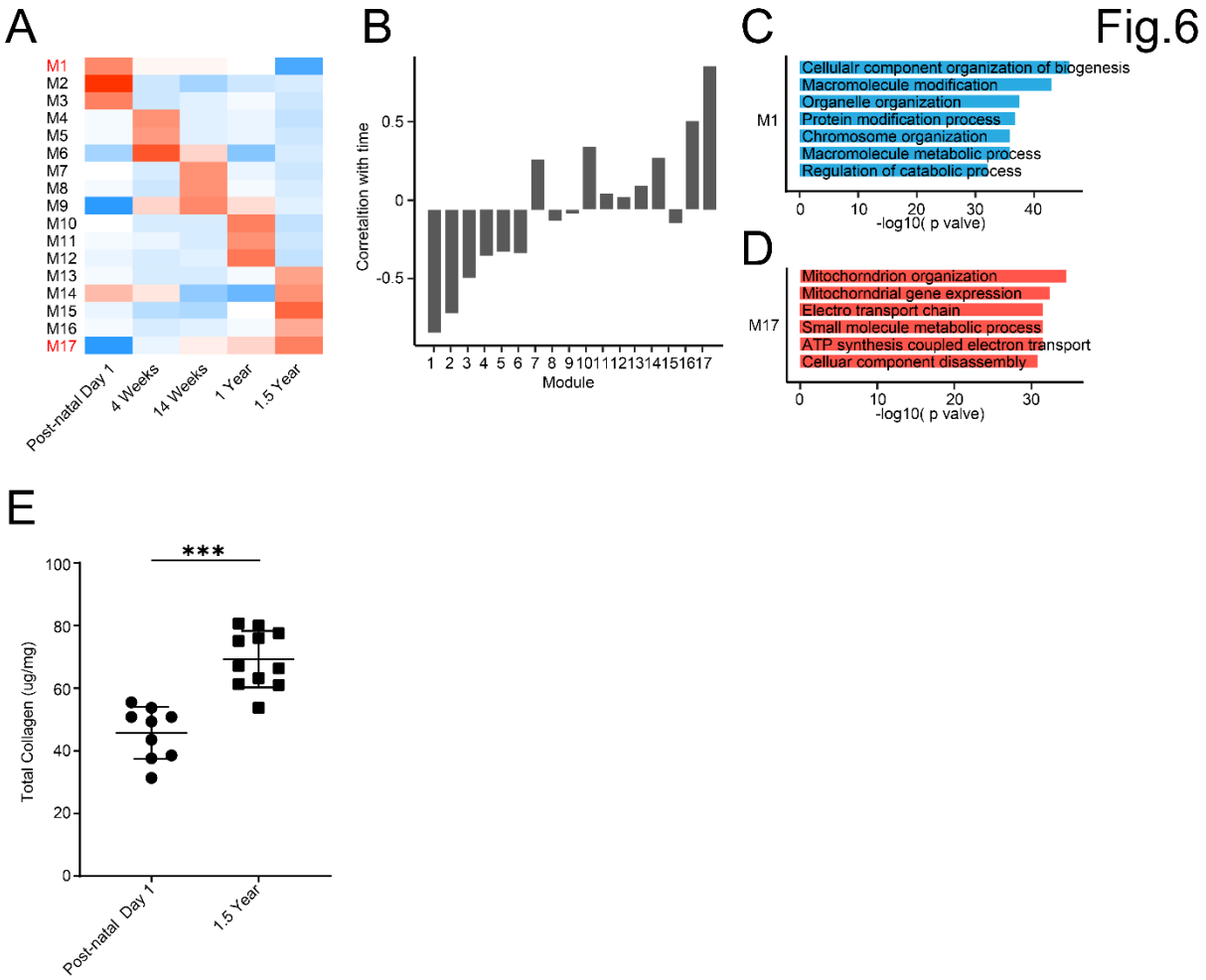

Figure 6. Transcriptional programs and collagen content of young and old hearts. (A) Hearts were harvested from post-natal day 1, 4 weeks, 14 weeks, 1 year and 1.5 year old animals and the heart tissue subjected to gene expression analysis by RNA-seq. **(A)** Weighted Gene Co-expression Network Analysis of Genes (WGCNA) was performed to identify modules of genes that correlated with time and a heat map demonstrates mean expression of these modules of genes in whole heart tissue with age. **(B)** Graphical representation demonstrating correlation of each module with time in the heart **(C,D)** Gene ontology analysis demonstrating principal pathways/biological processes that are **(C)** downregulated or **(D)** upregulated with age in module M1 or module M17 respectively. **(E)** Total collagen content of hearts of post-natal day 1 and 1.5 year old animals, expressed as unit weight of heart tissue (mean ± S.D ; ***p<0.001, 2-tailed Student's t test)

A

Fig.S1

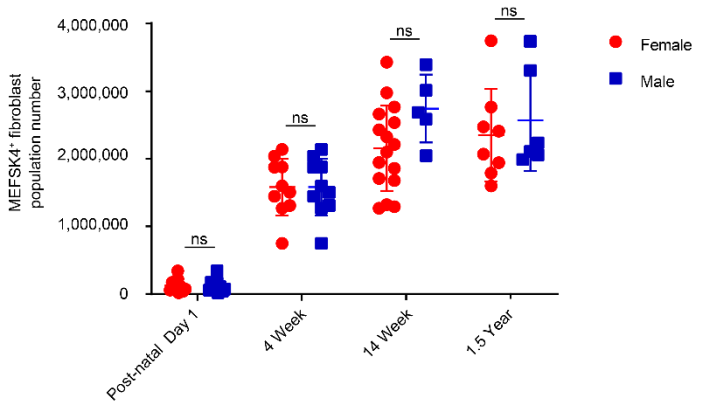

B

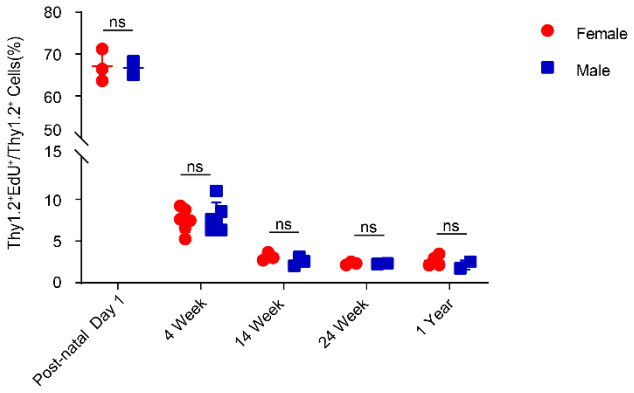

Supplementary Figure 1. Absolute cardiac fibroblast numbers and fibroblast proliferation rates in male and female mice of different ages. (A) Hearts were harvested from male and female mice of different ages and absolute cardiac fibroblast numbers measured between male and female hearts at each age (Neonatal n=11 Females and10 Males; 4 weeks n=10 Females and 10 Males; 14 weeks n=16 Female and 5 Males; 1.5 years n=8 Females and 6 Males; mean ± S.D.; ns= p>0.05). **(B)** Both male and female mice of different ages were injected with EdU (daily for 1 week) followed by harvesting of hearts and determination of numbers of Thy1.2EdU+ cells as a fraction of Thy1.2 cells in male and female hearts (Neonatal n=3 Females and 2 Males; 4 weeks n= 6 Females and 6 Males; 14 weeks n=3 Females and 3 Males; 24 weeks n=3 Females and 2 Males; 1.5 year n= 4 Females and 2 Males; mean ± S.D.; ns= p>0.05) Data analysis was performed by 1-way ANOVA with multiple-comparisons correction.

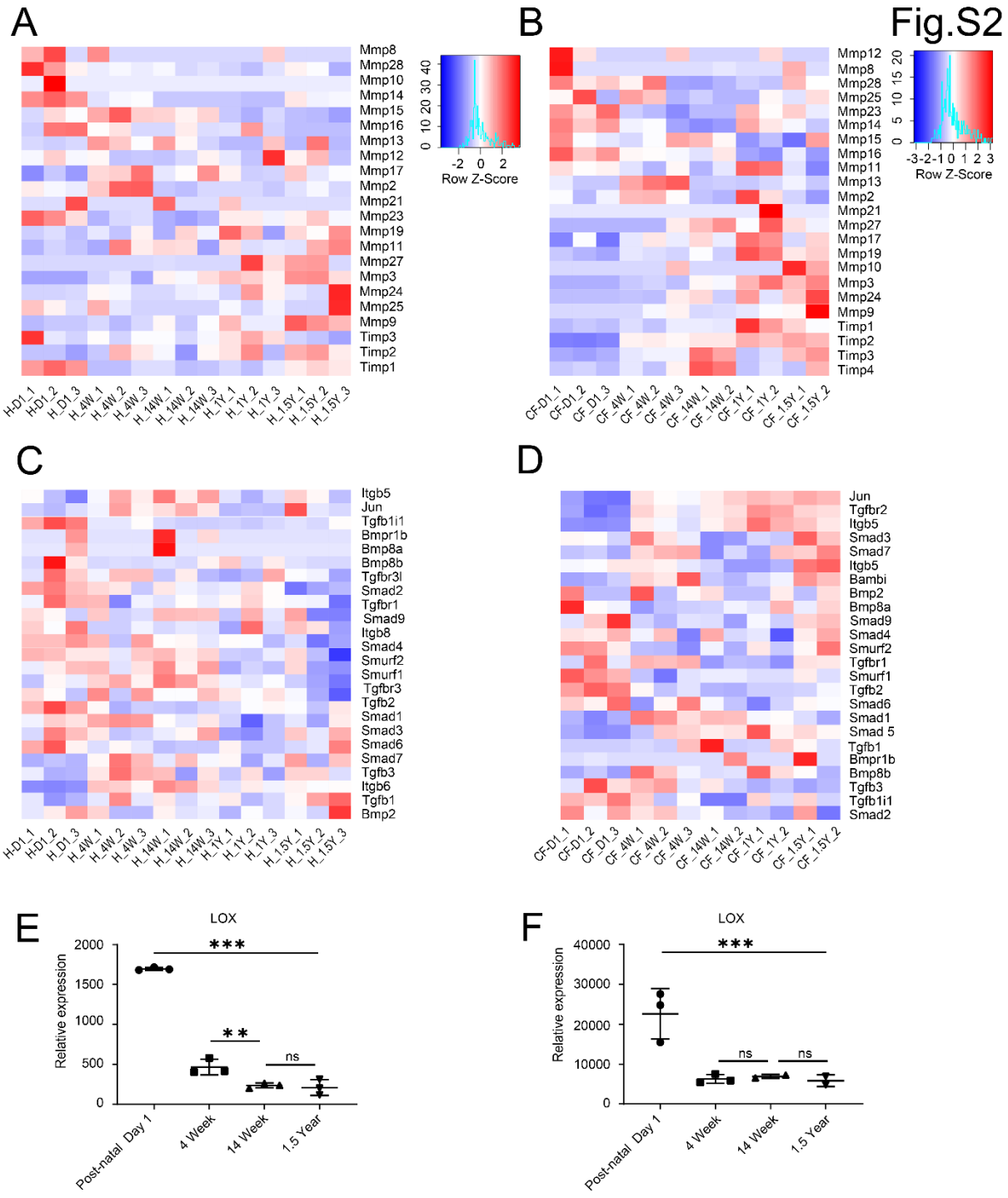

Supplementary Figure 2. **Temporal changes in heat expression of MMP, TIMP and LOX in hearts and cardiac fibroblasts of mice of different ages**. **(A,B)** Heat map demonstrating expression of members of the MMP family in **(A)** hearts and **(B)** cardiac fibroblasts isolated from hearts of mice at different ages (H: Heart CF: Cardiac fibroblasts). **(C,D)** Heat map demonstrating expression of members of the TGF-β signaling pathway in **(C)** hearts and **(D)** cardiac fibroblasts isolated from hearts of mice of different ages. (H: Heart CF: Cardiac fibroblasts). **(E,F)** Gene expression of lysyl oxidase (LOX) in hearts and cardiac fibroblasts isolated from hearts of mice of different ages (mean ± S.D.; *** p<0.0001, **p<0.01, ns= p>0.05). Data analysis was performed by 1-way ANOVA with multiple-comparisons correction.

Table 1. Highly correlated genes in fibroblast module 3

Term name	Gene
Cell cycle	*Eif4g1 Ilk Myh10 Ttc28 Top2b Hcfc1 Ccnd1 Tnks Ddx39b*
DNA replication	*Nfia Cdk2 Pola2 Nucks1 Mcm7 Orc6 Rtel1 Rev3l Atrx*
Spliceosome	*Rbm17 Lsm6 Rbmxl1 Ddx39b Snrnp70 Eif4a3 Prpf40a*
RNA transport	*Hnmpu Tnks Cpsf2 Ddx39b Ckap5 Khdrbs1 Srsf1 Wdr33*
Mismatch repair	*Mlh1 Tdg Exo1 Msh6 Setd2 Lig1 Abl1 Rpa2 Pold1 Mcm9*
Ubiquitin mediated proteolysis	*Pias2 Cdc26 Ube2c Skp2 Cdc16 Brca1 Ddb1 Vhl Cdc27*
Proteasome	*Psmc1 Psmd12 Psmb7 Psmc3 Psme4 Psmc4 Psmd8*

Table 2. Highly correlated genes in fibroblast module 17

Term name	Gene
Metabolic pathways	*Hexb Idua Inmt Gldc P4ha1 Adcy5 Sirt2 Gaa*
Lysosome	*Nagpa Hexb Lamp1 Ctsb Sumf1 Laptm4a Psap Gns*
Protein processing in endoplasmic reticulum	*Os9 Dnajb1 Sec62 Rpn2 Dnajb2 Ern1 Rad23a Hsph1*
Pathway in cancer	*Il7 Gng4 Adcy5 Gsta3 Stat3 Ptgs2 Gstp1 Dapk1 Mgst1*
MAPK signaling pathway	*Rasgrf1 Hspb1 Angptl1 Csf1 Nfkb1 Vegfd Ngf Tnfrsf1a*
AGE-RACE signaling pathway in diabetic complication	*Icam1 Egr1 Stat3 Nox4 Nfkb1 Stat5a Vegfd F3 jUN*
TNF signaling pathway	*Cx3cl1 Icam1 Mmp3 Cxcl1 Cxcl5 Ptgs2 Il6 Csf1 Socs3 Nfkb1*

Table 3. Highly correlated genes in Heart Module 1

Term name	Gene
Cellular component organization or biogenesis	*Col4a5 Kdm5b Scaf8 Synpo2l Kctd3 Pxdn Ccnf Tnks*
Macromolecule modification	*Klhdc10 Ccnf Ptpn9 Ror1 Nup188 Atxn7l3 Csnk1g3 Sptan1*
Organelle organization	*Synpo2l Tnks Myh10 Sptan1 Kdm6b Kit Dnmt3a*
Cellular protein modification process	*Klhdc10 Ptpn9 Ror1 Nup188 Atxn7l3 Csnk1g3 Sptan1*
Chromosome organization	*Atxn7l3 Kdm6b Dnmt3a Mki67 Tet3 Rad21 Chd4 Tet1*
Macromolecule metabolic process	*Kdm5b Klhdc10 Elf2 Tox2 Maz Adamts12 Tnks Ccnf Ror1*
Regulation of catabolic process	*Nup188 Ago2 Mtmr2 Nedd4 Itgb1 Foxk1 Nedd4l Abl1*

Table 4. Highly correlated genes in Heart Module 17

Term name	Gene
Mitochondrial gene expression	*Mrps21 Mrpl30 Mrpl28 Ndufa7 Mrpl42 Chchd1 Mtg2*
Mitochondrion organization	*Apoo Tmem70 Immp1l Ndufb3 Sdhaf4 Bnip3 Atp5j*
Electron transport chain	*Iscu Ndufb3 Ndufa6 Cox7b Immp2l Ndufa7 Uqcrb*
Small molecule metabolic process	*Gpx4 Iscu Nr1h3 Nudt7 Isca2 Gstm2 Acot13 Bdh1 Atp5j*
ATP synthesis coupled electron transport	*Iscu Danjc15 Ndufa5 Cox7b Ndufa7 Ndua12 Uqcrb*
Cellular component disassembly	*Mrps36 Mrpl Snapin Bnip3 Mrpl30 Mrpl42 Mmp3*

Supplementary Table 1

REAGENT or RESOURCE	SOURCE	IDENTIFIER
Antibodies		
MEFSK4-APC	Miltenyi Biotec	130-102-302
PDGFR-a-APC antibody	eBioscience	17-1401-81
Thy1.2-APC antibody	eBioscience	17-0902-82
CD31-APC antibody	eBioscience	17-0311-82
Ki 67-488 antibody	eBioscience	11-5698-82
Critical Commercial Kit and Reagent		
Permeabilization Buffer	eBioscience	00-8333-56
Click-iT™ Edu Alexa Fluor 488 flow cytometry assay kit	Invitrogen	C10425
Edu	Carbosynth,	NE0870
Calibration Particles	BD Sphero	556298
Sircol Soluble Collagen Assay Kit	Biocolor	S1000
Sircol Insoluble Collagen Assay Kit	Biocolor	S2000
Qiagen All prep DNA/RNA mini kit	Qiagen	80204